Supplemental Material for Efficient preparation of Dicke states

Jeffery Yu,[1,2,3] Sean R. Muleady,[1,2,*] Yu-Xin Wang (王语馨),[1,*]
Nathan Schine,[2,3] Alexey V. Gorshkov,[1,2] and Andrew M. Childs[1,4]

[1] *Joint Center for Quantum Information and Computer Science, NIST/University of Maryland, College Park, Maryland 20742, USA*
[2] *Joint Quantum Institute, NIST/University of Maryland, College Park, Maryland 20742, USA*
[3] *Department of Physics, University of Maryland, College Park, Maryland 20742, USA*
[4] *Department of Computer Science and Institute for Advanced Computer Studies, University of Maryland, College Park, Maryland 20742, USA*

Here, we provide additional details and calculations for the results stated in the main text. In Appendix A, we provide a rigorous derivation for the $O(\log j)$ runtime scaling of Theorem 1. In Appendix B, we elaborate on the robustness of the protocol and its efficient runtime against finite errors and discuss two representative error models. In both cases, the $O(\log j)$ runtime scaling is preserved under small errors.

CONTENTS

Appendix A: Asymptotic expansions of Wigner d-matrices

In this section, we rigorously analyze the time to prepare the $m_t = 0$ Dicke state. We proceed via three lemmas.

Lemma 1. *Starting from $m = j$, we can obtain a state with $|m'| \le \sqrt{j}$ in expected $O(1)$ time.*

Proof. From $m = j$, we rotate by $\theta_j = \frac{\pi}{2}$, which gives the state

$$e^{-i(\pi/2)J_y}\,|j,j\rangle = \left(\frac{|0\rangle + |1\rangle}{\sqrt{2}}\right)^{\otimes n} = \frac{1}{2^{n/2}} \sum_{x\in\{0,1\}^n} |x\rangle\,. \tag{S1}$$

The probability of measuring weight w is $\binom{n}{w}/2^n$, which is a binomial distribution with mean $\frac{n}{2}$ and variance $\frac{n}{4}$. If $|m'| > \sqrt{j}$, then the difference between w and the mean is of the same order as the standard deviation, so that the probabilities of those instances sum up to a bounded $O(1)$ probability, independent of n. In such a case, we simply reset and try again. The expected number of attempts to succeed is $O(1)$. □

Lemma 2. *In the regime $m = \omega(1)$, $m = O(\sqrt{j})$, and $0 < m' < 2m$, we have*

$$d^j_{m'm}(\beta_m) = \sqrt{\frac{2}{\pi m}}\,\frac{\cos\left[m(1-x)\arccos(1-x) - m\sqrt{1-(1-x)^2} + \frac{\pi}{4}\right]}{\left[1-(1-x)^2\right]^{\frac{1}{4}}} + O(\max\{m^2 j^{-2}, m^{-1}j^{-1}\}), \tag{S2}$$

where $\beta_m = \arcsin(m/j)$ and $x = m'/m$.

Proof. We start by rewriting the Wigner d-matrix element as the following integral (see Eq. (11) in Sec.4.3.3 of [S1]):

$$\begin{aligned} d^j_{m'm}(\beta_m) = {} & \frac{(-1)^{m'-m}}{2\pi}\left[\frac{(j+m')!(j-m')!}{(j+m)!(j-m)!}\right]^{\frac{1}{2}} \\ & \times \int_0^{2\pi} \left(e^{i\frac{\phi}{2}}\cos\frac{\beta_m}{2} + ie^{-i\frac{\phi}{2}}\sin\frac{\beta_m}{2}\right)^{j-m}\left(e^{-i\frac{\phi}{2}}\cos\frac{\beta_m}{2} + ie^{i\frac{\phi}{2}}\sin\frac{\beta_m}{2}\right)^{j+m} e^{im'\phi}\,\mathrm{d}\phi\,. \end{aligned} \tag{S3}$$

By shifting the integration variable $\phi \to \phi + \frac{\pi}{2}$, we can equivalently write this as

$$d^j_{m'm}(\beta_m) = \frac{(-1)^{m'-m}}{2\pi}\left[\frac{(j+m')!(j-m')!}{(j+m)!(j-m)!}\right]^{\frac{1}{2}} \times \int_0^{2\pi}\left(\cos\frac{\beta_m}{2} + e^{-i\phi}\sin\frac{\beta_m}{2}\right)^{j-m}\left(\cos\frac{\beta_m}{2} - e^{i\phi}\sin\frac{\beta_m}{2}\right)^{j+m} e^{i(m'-m)\phi}\,\mathrm{d}\phi\,. \tag{S4}$$

We now focus on the integrand, which can be split into the product of a positive magnitude and a phase part:

$$d^j_{m'm}(\beta_m) = \frac{(-1)^{m'-m}}{2\pi}\left[\frac{(j+m')!(j-m')!}{(j+m)!(j-m)!}\right]^{\frac{1}{2}} \int_0^{2\pi} g(\phi)e^{if(\phi)}\,\mathrm{d}\phi\,, \tag{S5}$$

$$g(\phi) = \exp\Big[\frac{j-m}{2}\log(1+\sin\beta_m\cos\phi) + \frac{j+m}{2}\log(1-\sin\beta_m\cos\phi)\Big], \tag{S6}$$

$$f(\phi) = (m'-m)\phi - (j-m)\arctan\frac{\sin\phi\tan\frac{\beta_m}{2}}{1+\cos\phi\tan\frac{\beta_m}{2}} - (j+m)\arctan\frac{\sin\phi\tan\frac{\beta_m}{2}}{1-\cos\phi\tan\frac{\beta_m}{2}}. \tag{S7}$$

We choose the rotation angle $\beta_m = \arcsin(m/j)$ according to the optimal angle predicted by the geometric picture, as discussed in the main text.

In order to make further approximations in the $j \to \infty$ limit, we first consider the derivatives of the functions $g(\phi)$ and $f(\phi)$ with respect to ϕ:

$$\frac{\mathrm{d}g(\phi)}{\mathrm{d}\phi} = -g(\phi)\sin\beta_m\sin\phi\frac{j\sin\beta_m\cos\phi + m}{1-\sin^2\beta_m\cos^2\phi}, \tag{S8}$$

$$\frac{\mathrm{d}f(\phi)}{\mathrm{d}\phi} = -(m-m') - \frac{(j-m)\tan\frac{\beta_m}{2}(\cos\phi+\tan\frac{\beta_m}{2})}{1+(\tan\frac{\beta_m}{2})^2+2\cos\phi\tan\frac{\beta_m}{2}} - \frac{(j+m)\tan\frac{\beta_m}{2}(\cos\phi-\tan\frac{\beta_m}{2})}{1+(\tan\frac{\beta_m}{2})^2-2\cos\phi\tan\frac{\beta_m}{2}}. \tag{S9}$$

For $m, m' = \omega(1)$ and $m = O(\sqrt{j})$, the magnitude function $g(\phi)$ varies much slower (by an extra factor of $\sin\beta_m = m/j$) relative to the phase function $f(\phi)$, and we can apply the stationary phase approximation to the integral in Eq. (S4). In this regime, noting that $\sin\beta_m = m/j$, the derivative of the phase function can be well approximated as

$$\frac{\mathrm{d}f(\phi)}{\mathrm{d}\phi} = -(m-m') - m\cos\phi[1+O(m^2j^{-2})], \tag{S10}$$

so that, under the stationary phase approximation (see Sec. 3 of Ref. [S2]), we have that in the $j \to \infty$ limit, with $m, m' = \omega(1)$ and $m = O(\sqrt{j})$, the following equation holds:

$$\int_0^{2\pi} g(\phi)e^{if(\phi)}\,\mathrm{d}\phi = \sum_{\phi_s=\pi\pm\arccos\frac{m-m'}{m}} g(\phi_s)e^{if(\phi_s)\pm i\frac{\pi}{4}}\sqrt{\frac{2\pi}{\left|\frac{d^2f(\phi)}{d\phi^2}\right|_{\phi=\phi_s}}} + O(\max\{m^2j^{-2}, m^{-1}j^{-1}\}). \tag{S11}$$

Substituting Eq. (S11) back into Eq. (S5), we obtain the desired approximate asymptotic expression for the Wigner d-matrix in this regime:

$$d^j_{m'm}(\beta_m) = \frac{\sqrt{\frac{2}{\pi}}\left[\frac{j^2-m'^2}{j^2-m^2}\right]^{\frac{1}{4}}}{[m^2-(m-m')^2]^{\frac{1}{4}}}\cos\left[(m-m')\arccos\frac{m-m'}{m} - \sqrt{m^2-(m-m')^2} + \frac{\pi}{4}\right] + O(\max\{m^2j^{-2}, m^{-1}j^{-1}\}). \tag{S12}$$

Rewriting with $x = m'/m$ gives the result. □

Note that, if $m' < 0$ or $m' > 2m$, then Eq. (S10) does not have a solution for $\phi \in [0, 2\pi]$, meaning that the d-matrix element is negligible up to leading order.

As shown in Sec. 4.18.1 of [S1], in the regime where $m = O(1)$ and $m = o(\sqrt{j})$, we have

$$\lim_{j\to\infty} d^j_{m'm}(\beta_m) = J_{m-m'}(m), \tag{S13}$$

where $J_\ell(x)$ is the Bessel function of the first kind. As the zeros of the Bessel function are transcendental [S3], we see that the asymptotic transition probabilities from m to m' are nonzero in this regime with $|d^j_{m'm}(\beta_m)|^2 = \Theta(1)$. This means that once we reach a transient state m with $m = O(1)$, it takes $O(1)$ steps to reach the final target state.

Define the random variable M by

$$M = \begin{cases} m & |m| \le \sqrt{j} \\ \sqrt{j}+1 & |m| > \sqrt{j}. \end{cases} \tag{S14}$$

This is a proxy for m. We also introduce M' as a function of m' in a similar fashion, as the reset drastically increases m' to j, making the expectations of $\langle m'^\alpha \rangle$ suboptimal for the runtime analysis.

Lemma 3. *There exists a constant $c < 1$ and positive exponent $0 < \alpha < 1$ such that, for every $m = \omega(1)$ and $m \le \sqrt{j}$,*

$$\sum_{m'} \left|d^j_{m'm}(\beta_m)\right|^2 \frac{M'^\alpha}{M^\alpha} < c. \tag{S15}$$

Proof. Now consider

$$\sum_{m'} \mathcal{P}(m \to m') \frac{M'^\alpha}{M^\alpha} = \frac{(1 - \sum_{m'<\sqrt{j}} |d^j_{m'm}(\beta_m)|^2)(\sqrt{j}+1)^\alpha + \sum_{m'<\sqrt{j}} |d^j_{m'm}(\beta_m)|^2 m'^\alpha}{m^\alpha}. \tag{S16}$$

We can make use of the asymptotic expression in Eq. (S12) to simplify this expression. We first note that, for $j \to \infty$ with $m, m' = \omega(1)$ and $m = O(\sqrt{j})$, the reset probability is given by

$$\begin{aligned} &1 - \sum_{m'<\sqrt{j}} |d^j_{m'm}(\beta_m)|^2 \\ &\quad = 1 - \frac{1}{\pi} \sum_{m'<\sqrt{j}} \left\{ \frac{1 + \sin\left[2(m-m') \arccos\frac{m-m'}{m} - 2\sqrt{m^2 - (m-m')^2}\right]}{\sqrt{m^2-(m-m')^2}} + O(\max\{m^2 j^{-2}, m^{-1} j^{-1}\}) \right\}. \end{aligned} \tag{S17}$$

In the large-j limit, we can further approximate this expression as an integral: making use of Eq. (S2), we have (henceforth still under the conditions $j \to \infty$, $m, m' = \omega(1)$, and $m = O(\sqrt{j})$)

$$\begin{aligned} &1 - \sum_{m'<\sqrt{j}} |d^j_{m'm}(\beta_m)|^2 \\ &\quad = 1 - \int_0^2 H\left(\frac{\sqrt{j}}{m} - x\right) \frac{1 + \sin\left[2m(1-x)\arccos(1-x) - 2m\sqrt{1-(1-x)^2} + \frac{\pi}{2}\right]}{\sqrt{1-(1-x)^2}} \frac{\mathrm{d}x}{\pi} + O(\max\{m^2 j^{-\frac{3}{2}}, m^{-1} j^{-\frac{1}{2}}\}) \\ &\quad = 1 - \int_0^2 H\left(\frac{\sqrt{j}}{m} - x\right) \frac{\mathrm{d}x}{\pi\sqrt{1-(1-x)^2}} + O(\max\{m^2 j^{-\frac{3}{2}}, m^{-1} j^{-\frac{1}{2}}\}). \end{aligned} \tag{S18}$$

Here, $H(\cdot)$ denotes the Heaviside step function. Now we divide the analysis of Eq. (S16) into two cases. First, if $m < \sqrt{j}/2$, then the step function is always 1, so the integral is $\int_0^2 \frac{\mathrm{d}x}{\pi\sqrt{1-(1-x)^2}} = 1$, and the reset probability in Eq. (S18) is negligible. In this case, Eq. (S16) gives

$$m < \sqrt{j}/2: \quad \sum_{m'} \mathcal{P}(m \to m') \frac{m'^\alpha}{m^\alpha} = \sum_{0 \le m' \le 2m} |d^j_{m'm}(\beta_m)|^2 \frac{m'^\alpha}{m^\alpha} + O(\max\{m^2 j^{-\frac{3}{2}}, m^{-1} j^{-\frac{1}{2}}\}). \tag{S19}$$

Substituting Eq. (S2) into the above equation, we obtain

$$\begin{aligned} m < \sqrt{j}/2: \quad &\sum_{m'} \mathcal{P}(m \to m') \frac{m'^\alpha}{m^\alpha} \\ &= \int_0^2 x^\alpha \frac{1 + \sin\left[2m(1-x)\arccos(1-x) - 2m\sqrt{1-(1-x)^2} + \frac{\pi}{2}\right]}{\sqrt{1-(1-x)^2}} \frac{\mathrm{d}x}{\pi} + O(\max\{m^2 j^{-\frac{3}{2}}, m^{-1} j^{-\frac{1}{2}}\}) \\ &= \int_0^2 \frac{x^\alpha \, \mathrm{d}x}{\pi\sqrt{1-(1-x)^2}} + O(\max\{m^2 j^{-\frac{3}{2}}, m^{-1} j^{-\frac{1}{2}}\}). \end{aligned} \tag{S20}$$

We can explicitly compute the integral on the right-hand side as

$$\int_0^2 \frac{x^\alpha \, \mathrm{d}x}{\pi\sqrt{1-(1-x)^2}} = \frac{1}{\pi}\int_0^\pi (1-\cos\theta)^\alpha \, \mathrm{d}\theta = \frac{2^\alpha}{\pi}\int_0^\pi \sin^{2\alpha}\frac{\theta}{2} \, \mathrm{d}\theta = \frac{2^\alpha}{\pi} B(\alpha+\tfrac{1}{2},\tfrac{1}{2}), \tag{S21}$$

where $B(\cdot,\cdot)$ denotes the beta function.

Noting that $\sin^{2\alpha}\frac{\theta}{2} < (\frac{\theta}{2})^{2\alpha}$ for all $\theta > 0$, we can upper bound Eq. (S21) as

$$\frac{2^\alpha}{\pi}\int_0^\pi \sin^{2\alpha}\frac{\theta}{2} \, \mathrm{d}\theta < \frac{2^\alpha}{\pi}\int_0^\pi \frac{\theta^{2\alpha}}{2^{2\alpha}} \, \mathrm{d}\theta = \frac{\pi^{2\alpha}}{2^\alpha(2\alpha+1)}. \tag{S22}$$

Expanding the function $\frac{\pi^{2\alpha}}{2^\alpha} - (2\alpha+1)$ in a Taylor series, it is straightforward to show that this expression is strictly smaller than 0 for $\alpha \in (0, 0.1)$, so for such values of α, $\pi^{2\alpha}/[2^\alpha(2\alpha+1)] < 1$, and therefore

$$m = \omega(1),\, m < \sqrt{j}/2: \quad \sum_{m'} \mathcal{P}(m\to m')\frac{m'^\alpha}{m^\alpha} < 1. \tag{S23}$$

(Alternatively, we show in the End Matter that Eq. (S21) is at most 1 for all $\alpha \in (0,1)$.)

In the other regime $m > \sqrt{j}/2$, we compute the contribution from the reset separately. In this case, from Eq. (S18), we can write the reset probability as

$$\sqrt{j} \geq m > \sqrt{j}/2: \quad 1 - \sum_{m'<\sqrt{j}} |d^j_{m'm}(\beta_m)|^2 = 1 - \int_0^{\frac{\sqrt{j}}{m}} \frac{\mathrm{d}x}{\pi\sqrt{1-(1-x)^2}} + O(\max\{m^3 j^{-2}, j^{-1}\}) \tag{S24}$$

$$= \frac{1}{2} - \frac{\arcsin(\frac{\sqrt{j}}{m}-1)}{\pi} + O(m^3 j^{-2}), \tag{S25}$$

so that, in this regime, we can derive an upper bound for Eq. (S16) as

$$\begin{aligned}
\sum_{m'} \mathcal{P}(m\to m')\frac{m'^\alpha}{m^\alpha} &< \left(\frac{1}{2} - \frac{\arcsin(\frac{\sqrt{j}}{m}-1)}{\pi} + O(m^3 j^{-2})\right)\frac{(\sqrt{j}+1)^\alpha}{m^\alpha} + \sum_{m'<\sqrt{j}} |d^j_{m'm}(\beta_m)|^2 \frac{m'^\alpha}{m^\alpha} \\
&= \left(\frac{1}{2} - \frac{\arcsin(\frac{\sqrt{j}}{m}-1)}{\pi} + O(m^3 j^{-2})\right)\left(\frac{\sqrt{j}}{m}\right)^\alpha \left(1 + O(j^{-\frac{1}{2}})\right) \\
&\quad + \int_0^{\frac{\sqrt{j}}{m}} x^\alpha \frac{1+\sin\left[2m(1-x)\arccos(1-x) - 2m\sqrt{1-(1-x)^2} + \frac{\pi}{2}\right]}{\sqrt{1-(1-x)^2}} \frac{\mathrm{d}x}{\pi} + O(m^3 j^{-2}) \\
&= \left(\frac{1}{2} - \frac{\arcsin(\frac{\sqrt{j}}{m}-1)}{\pi}\right)\left(\frac{\sqrt{j}}{m}\right)^\alpha + \int_0^{\frac{\sqrt{j}}{m}} \frac{x^\alpha \, \mathrm{d}x}{\pi\sqrt{1-(1-x)^2}} + O(m^{3-\alpha} j^{-2+\frac{\alpha}{2}}) \\
&= \left(\frac{1}{2} - \frac{\arcsin(\frac{\sqrt{j}}{m}-1)}{\pi}\right)\left(\frac{\sqrt{j}}{m}\right)^\alpha + \frac{1}{\pi}\int_0^{\pi-\arccos(\frac{\sqrt{j}}{m}-1)} (1-\cos\theta)^\alpha \, \mathrm{d}\theta + O(m^{3-\alpha} j^{-2+\frac{\alpha}{2}}) \\
&= \frac{\arccos(\frac{\sqrt{j}}{m}-1)}{\pi}\left(\frac{\sqrt{j}}{m}\right)^\alpha + \frac{2^\alpha}{\pi}\int_0^{\pi-\arccos(\frac{\sqrt{j}}{m}-1)} \sin^{2\alpha}\frac{\theta}{2} \, \mathrm{d}\theta + O(m^{3-\alpha} j^{-2+\frac{\alpha}{2}}) \\
&< \frac{\arccos(\frac{\sqrt{j}}{m}-1)}{\pi}\left(\frac{\sqrt{j}}{m}\right)^\alpha + \frac{\left[\pi - \arccos(\frac{\sqrt{j}}{m}-1)\right]^{2\alpha+1}}{\pi(2\alpha+1)2^\alpha} + O(m^{3-\alpha} j^{-2+\frac{\alpha}{2}}).
\end{aligned} \tag{S26}$$

We can show that the right-hand side of Eq. (S26) is again asymptotically upper bounded by a number smaller than 1. Specifically, setting $\arccos(\frac{\sqrt{j}}{m}-1) = \zeta$, we can rewrite the first two terms in Eq. (S26) as

$$\frac{\zeta}{\pi}(1+\cos\zeta)^\alpha + \frac{(\pi-\zeta)^{2\alpha+1}}{\pi(2\alpha+1)2^\alpha}, \quad \zeta \in \left(0, \frac{\pi}{2}\right). \tag{S27}$$

For $\alpha \in (0,1)$, the function in Eq. (S27) monotonically decreases as ζ increases, so that

$$\zeta \in (0, \frac{\pi}{2}): \quad \frac{\zeta}{\pi}(1+\cos\zeta)^\alpha + \frac{(\pi-\zeta)^{2\alpha+1}}{\pi(2\alpha+1)2^\alpha} \leq \frac{\pi^{2\alpha}}{(2\alpha+1)2^\alpha}. \tag{S28}$$

From our upper bound on Eq. (S22), this is at most 1 for $\alpha \in (0, 0.1)$, so we obtain

$$\sqrt{j} \geq m > \sqrt{j}/2: \quad \frac{\arccos(\frac{\sqrt{j}}{m}-1)}{\pi}\left(\frac{\sqrt{j}}{m}\right)^\alpha + \frac{\left[\pi - \arccos(\frac{\sqrt{j}}{m}-1)\right]^{2\alpha+1}}{\pi(2\alpha+1)2^\alpha} < 1 \quad \forall \alpha \in (0, 0.1). \tag{S29}$$

Further, noting that $m \leq \sqrt{j}$, we see that in the asymptotic $j \to \infty$ limit, the last term in Eq. (S26), $O(m^{3-\alpha} j^{-2+\frac{\alpha}{2}})$, becomes $o(1)$, as

$$m^{3-\alpha} j^{-2+\frac{\alpha}{2}} = \left(\frac{m}{\sqrt{j}}\right)^{3-\alpha} j^{-\frac{1}{2}} \leq j^{-\frac{1}{2}}. \tag{S30}$$

Thus, we have shown that, in the asymptotic limit $j \to \infty$, the following inequality holds for every m satisfying $m = \omega(1)$ and $m = O(\sqrt{j})$:

$$\sum_{m'} \mathcal{P}(m \to m') \frac{m'^\alpha}{m^\alpha} < 1, \quad \forall \alpha \in (0, 0.1). \tag{S31}$$

Choosing any particular $\alpha \in (0, 0.1)$ gives the result. □

Proof of Theorem 1. At time 0, we have $m = j$ with probability 1, so $\langle [M(0)]^\alpha \rangle = (\sqrt{j}+1)^\alpha$, where we define $M(t)$ as a function of m at time step t as per Eq. (S14). By Lemma 3, we have $\frac{\langle [M(t+1)]^\alpha \rangle}{\langle [M(t)]^\alpha \rangle} < c$ for each t with $M(t) = \omega(1)$, so

$$\langle [M(t)]^\alpha \rangle < c^t \langle [M(0)]^\alpha \rangle = c^t (\sqrt{j}+1)^\alpha, \tag{S32}$$

unless there exists a $t' \leq t$ such that $M(t') = O(1)$. Making use of the above inequality, for any desired $\varepsilon > 0$, we can attain either $\langle [M(t)]^\alpha \rangle < \varepsilon$ or $M(t) = O(1)$ in time

$$t_\varepsilon = \frac{\alpha \log(\sqrt{j}+1) + \log(1/\varepsilon)}{\log(1/c)} = O(\log j). \tag{S33}$$

In the former case, we have

$$t \geq t_\varepsilon: \quad \varepsilon > \langle [M(t)]^\alpha \rangle \geq \Pr[M(t)=0] \cdot 0 + \Pr[M(t) \geq 1] \cdot 1 = \Pr[M(t) \geq 1] = 1 - \Pr[M(t) = 0], \tag{S34}$$

so that $\Pr[M(t) = 0] > 1 - \varepsilon$. In the latter case, i.e., if we have $M(t) = O(1)$, from Eq. (S13) we conclude that any such state has a $\Theta(1)$ transition probability to reach the $m = 0$ state. Thus in expectation repeating this $O(\log j)$-step procedure a constant number of times will yield the $m = 0$ state. □

Appendix B: Effect of different error models on the performance and runtime of the Dicke state preparation protocol

Here, we examine the robustness of our state preparation protocol to measurement error. We focus on two distinct, simplified error models, motivated by typical error sources present in cavity QED setups that directly affect our proposed J_z measurements in this context.

In both error models we consider, the ability to directly prepare a pure Dicke state via our protocol is ultimately limited to some fidelity $1 - p$ for $p > 0$, where the state following a measurement is either a coherent superposition or incoherent mixture of Dicke states with some normally distributed weights about the inferred value of m. This translates to a limit on the fidelity of the final prepared state, regardless of the number of steps employed in our algorithm. However, for certain contexts—particularly quantum sensing and metrology—one is not necessarily interested in preparing an exact Dicke state, but rather obtaining a state with a sufficiently narrow distribution of m

about target $m_t = 0$. In both cases, it is thus of interest to compute how quickly our algorithm converges to the best attainable proxy state for $|m_t\rangle$.

a. *Finite detection efficiency model*

For our first error model, we set the state following an inferred J_z measurement outcome of m to be

$$\hat{\rho}_m \propto \sum_{m'=-j}^{j} e^{-(m-m')^2/2\sigma^2} |m'\rangle \langle m'|, \tag{S1}$$

where $\sigma > 0$ is the resulting distribution width. For a preparation of the target Dicke state with $m_t = 0$, our goal within this model is to prepare the state $\hat{\rho}_0$, which has fidelity $1 - p = (\sum_{m=-j}^{j} e^{-m^2/2\sigma^2})^{-1}$ to $|m_t = 0\rangle$.

Physically, this corresponds to a measurement process in which our state is perfectly projected onto a Dicke state, but our knowledge regarding the final measurement outcome is imprecise. For transmission-based readout schemes in cavity QED systems, one effect leading to this type of error is an imperfect photon collection efficiency $\eta_{\mathrm{ph}} < 1$ at the cavity output, where photons encoding information about the projected state are sometimes missed in detection. Here η_{ph} is the probe light transmission probability when its frequency is resonant with the vacuum Rabi frequency of the measured spin state, ω_{m_0}. Generically for an off-resonant probe, the transmission probability becomes $\eta_{\mathrm{ph}} T_{m_0}[\omega_m]$, where $T_{m_0}[\cdot]$ is the transmission function of the spin state, and ω_m is the probe frequency.

In this case, we can phenomenologically incorporate this effect into our model in Eq. (S1) by setting $\sigma^2 \sim 1/(n_{\mathrm{ph}}\eta_{\mathrm{ph}})$, for n_{ph} collected probe photons [S4]. In Fig. S1(a), we plot the expected number of steps for the preparation of $\hat{\rho}_{m_t=0}$ via our protocol for a range of σ and system sizes n, where for simplicity, we do not include resets in the protocol. We observe that even for $\sigma \sim 1$, where each $\hat{\rho}_m$ has a significant overlap with the states $|m \pm 1\rangle$, the increase in the expected number of steps is marginal.

We may also analyze the effect of finite detection efficiency on our ability to infer the measurement outcome within our proposed multichromatic interferometer, introduced in the main text. We operate in the regime where the smallest difference between neighboring transmission resonances is much greater than the peak linewidth, $g/\sqrt{n} \gg \kappa$, where n is the total atom number, such that $T_{m_0}[\omega_m] \ll 1$ whenever $m \neq m_0$. After the heterodyne step, the goal is to identify the resonant probe tone with the vacuum Rabi frequency. This is a hypothesis testing problem with the goal of distinguishing between two possible transmission coefficients, η_{ph} ($m = m_0$) versus $\eta_{\mathrm{ph}} T_{m_0}[\omega_m]$ ($m \neq m_0$) for each m. Upon collecting n_{ph} photons at frequency ω_m, the failure probability of hypothesis testing, i.e., the error probability in the total spin state detection, decays exponentially in n_{ph}. We see that this measurement scheme requires $g/\sqrt{n} \gg \kappa$, corresponding to a cooperativity between the atomic ensemble and the cavity that scales as n, in which case the measurement error probability is exponentially suppressed when collecting more photons at the output.

We can also directly examine the effect of finite detection efficiency on the scaling of the number of steps used by our preparation scheme. In this case, we can show that the same runtime scaling $O(\log j)$ still applies, by considering a slightly modified version of the proof in the above section. In the presence of an error probability p, we denote the transition probability as $\mathcal{P}_{\mathrm{meas}}(m \to m')$, so that we have

$$\sum_{m'} \mathcal{P}_{\mathrm{meas}}(m \to m') \frac{M'^{\alpha}}{M^{\alpha}} \leq \sum_{m'} \mathcal{P}(m \to m') \frac{(M' + Cp)^{\alpha}}{M^{\alpha}} < \sum_{m'} \mathcal{P}(m \to m') \frac{M'^{\alpha}}{M^{\alpha}} (1 + Cp)^{\alpha}, \tag{S2}$$

where C is a positive constant denoting the uncertainty in the total spin projection due to measurement errors. We have thus shown that there exists a small probability p_{th}, such that for any $p < p_{\mathrm{th}}$, $\sum_{m'} \mathcal{P}_{\mathrm{meas}}(m \to m') \frac{M'^{\alpha}}{M^{\alpha}} < 1$, and we can again use an argument similar to Eq. (S34) to show that the runtime to reach the final state (with an $O(p)$ infidelity with the ideal target Dicke state) is $O(\log j)$.

b. *Finite cooperativity model*

For our second error model, we instead let the state following an inferred J_z measurement outcome of m be (see, e.g., [S5])

$$|\psi_m\rangle \propto \sum_{m'} e^{-(m-m')^2/4\sigma^2} |m'\rangle, \tag{S3}$$

where $\sigma > 0$ is again the resulting distribution width. For a preparation of the target Dicke state with $m_t = 0$, our goal is now to prepare the state $|\psi_0\rangle$, which has the same fidelity to the target Dicke state $|m_t = 0\rangle$ as in our finite detection efficiency model for corresponding values of σ.

Within this model, our state is imperfectly projected into a given Dicke state, resulting in a conditional spin-squeezed state with reduced J_z variance. In the cavity QED context, this models the effect of a finite cavity cooperativity, in conjunction with a finite number of collected photons; however, we assume that all such photons are detected with unit efficiency. For (single-atom) cooperativity $C = 4g^2/\Gamma\kappa$ and number of collected probe photons n_{ph}, we can model this via Eq. (S3) with $\sigma^2 \sim (\delta/C\Gamma)^2/n_{\mathrm{ph}}$ [S4, S6, S7]. As more photons are collected, the J_z variance of the resulting state becomes increasingly squeezed; however, spontaneous emission of photons by the atoms into free space at rate Γ sets a fundamental limit on the squeezing of the final state. In the optimal case, and neglecting imperfect detection efficiency, the variance is bounded from below by $\sigma^2 \sim \sqrt{N/C}$, though in practice, the resulting state may not be pure as assumed in our model.

In Fig. S1(b), we plot the expected number of steps for the preparation of $|\psi_0\rangle$ via our protocol, where we again do not include resets. However, we make the crucial modification that we perform our global rotations about the x axis, rather than y, as interference effects from our superposition can significantly alter the resulting transition probability matrix with the latter choice. While there is a noted increase in the number of steps as σ increases compared to Fig. S1(a), the curves appear to generally retain a logarithmic growth (represented by straight lines on the semi-logarithmic plot). We note that at smaller n, when σ is roughly the same order of magnitude as n, the number of steps grows linearly with n. This occurs since the state following any given measurement is essentially an equal superposition of all possible Dicke states; thus, the chance to prepare m_t at any stage of the protocol is always $\sim 1/n$, resulting in an expected number of steps $\sim n$.

c. *Further discussion*

In a sense, Fig. S1 shows the worst-case performance of our algorithm for each error model. A given cavity QED setup will generally involve some combination of these two error sources. Since the resulting σ for the considered finite detection efficiency and finite cooperativity are both highly dependent on the number of collected photons, and thus depend on the measurement time for each mid-circuit measurement, it may be possible to achieve improved performance by utilizing variable, optimized measurement times at each stage of the protocol based on the specific cavity parameters. In addition, practical performance enhancements can be achieved by the inclusion of resets in either error model.

In both of the above models, as σ sets the precision with which individual Dicke states might be resolved from their neighbors, it is less likely that one actually desires the exact state $\hat{\rho}_0$ or $|\psi_0\rangle$, particularly for metrology and sensing tasks. Rather, a sufficient condition for the success of our preparation scheme is the detection of any m within a distance $\sim \sigma$ of $m_t = 0$. This will generally reduce the expected number of steps for the completion of our algorithm.

---

* These two authors contributed equally.

[S1] D. A. Varshalovich, A. N. Moskalev, and V. K. Khersonskii, Wigner d-functions, in *Quantum Theory of Angular Momentum* (World Scientific, 1988) Chap. 4, pp. 72–129.

[S2] R. Wong, Classical procedures, in *Asymptotic Approximations of Integrals*, Classics in Applied Mathematics No. 34 (SIAM, 2001) Chap. 2, pp. 55–146.

[S3] C. L. Siegel, Über einige Anwendungen diophantischer Approximationen, Sitzungsberichte der Preußischen Akademie der Wissenschaften, Math.-Phys. Klasse **1**, 81 (1929).

[S4] M. H. Schleier-Smith, I. D. Leroux, and V. Vuletić, States of an Ensemble of Two-Level Atoms with Reduced Quantum Uncertainty, Physical Review Letters **104**, 073604 (2010).

[S5] K. Jacobs and D. A. Steck, A straightforward introduction to continuous quantum measurement, Contemp. Phys. **47**, 279 (2006).

[S6] L. B. Madsen and K. Mølmer, Spin squeezing and precision probing with light and samples of atoms in the Gaussian description, Physical Review A **70**, 052324 (2004).

[S7] J. Appel, P. J. Windpassinger, D. Oblak, U. B. Hoff, N. Kjærgaard, and E. S. Polzik, Mesoscopic atomic entanglement for precision measurements beyond the standard quantum limit, Proceedings of the National Academy of Sciences **106**, 10960 (2009).

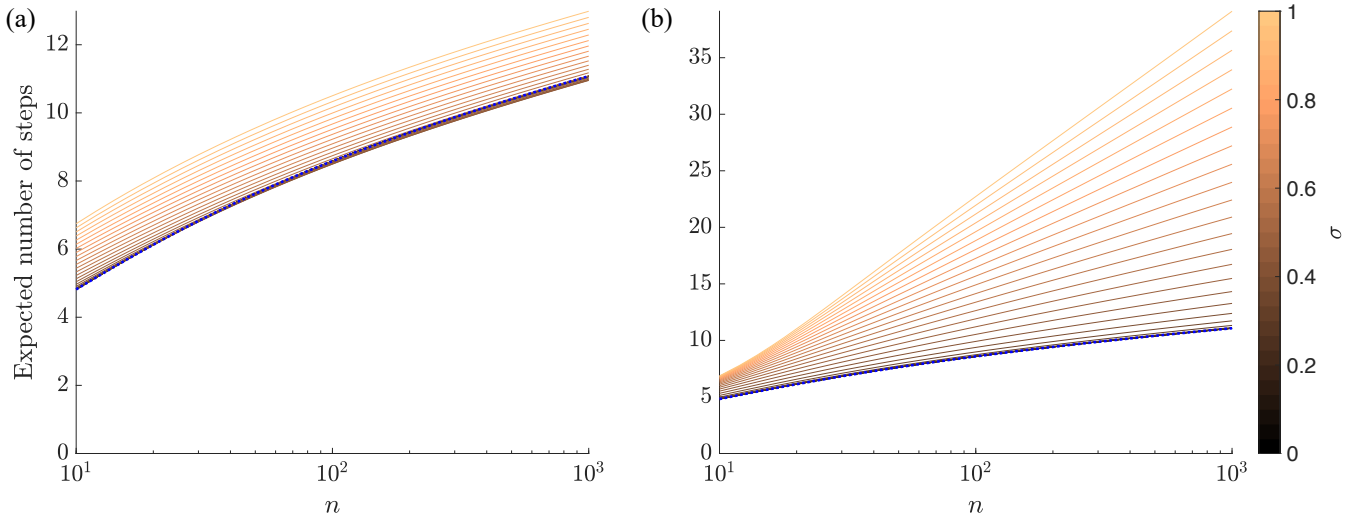

FIG. S1. Analysis of the effect of different measurement errors on our protocols. We plot the expected number of steps for our algorithm to yield a measurement of the $m_t = 0$ Dicke state, for a range of system sizes n and widths σ representing the distribution of our state about the inferred outcome of each J_z measurement. We examine the case where our state takes the form of an (a) incoherent mixture or (b) coherent superposition of Dicke states following each measurement. Within the context of cavity transmission-based readout schemes, these respectively model the effect of a) finite photon detection efficiency or b) a finite cooperativity in combination with a finite number of emitted photons. The blue dotted line in each panel corresponds to the ideal protocol.